Identification of a convergent spinal neuron population that encodes itch

Tayler D. Sheahan[1,6,*], Charles A. Warwick[1,6], Abby Y. Cui[1], David A.A. Baranger[2], Vijay J. Perry[1], Kelly M. Smith[1,3], Allison P. Manalo[1,4], Eileen K. Nguyen[1,3], H. Richard Koerber[1], Sarah E. Ross[1,7,*]

Author affiliations
[1] Pittsburgh Center for Pain Research and Department of Neurobiology, University of Pittsburgh, Pittsburgh, Pennsylvania, USA
[2] Department of Psychological and Brain Sciences, Washington University in St. Louis, St. Louis Missouri, USA
[3] Current Address: Biohaven Pharmaceuticals, LTD, Pittsburgh, Pennsylvania, USA
[4] Current Address: Department of Perioperative Medicine, Clinical Center, National Institutes of Health, Bethesda, Maryland, USA
[5] Current Address: Department of Anesthesiology and Perioperative Care, University of California, Los Angeles, Los Angeles, California, USA
[6] Co-first authors
[7] Lead contact
* Correspondence: tayler.sheahan@pitt.edu (T.D.S), saross@pitt.edu (S.E.R.)

In brief
Sheahan et al. identify a convergent population of spinal neurons that encodes diverse itch stimuli and find that GRPR spinoparabrachial neurons convey itch to the brain.

Highlights
- A convergent population of spinal neurons defined by the expression of GRPR encodes diverse itch stimuli
- GRPR spinal projection neurons transmit itch from the spinal cord to the lateral parabrachial nucleus
- GRPR activation elicits intrinsic Ca^{2+} oscillations

Summary
Itch is a protective sensation that drives scratching. Although specific cell types have been proposed to underlie itch, the neural circuit basis for itch remains unclear. Here, we used two-photon Ca^{2+} imaging in the dorsal horn to visualize the neuronal populations that are activated by itch-inducing agents. We identify a convergent population of spinal neurons that is defined by the expression of GRPR. Moreover, we discover that itch is conveyed to the brain via GRPR-expressing spinal output neurons that target the lateral parabrachial nucleus. Finally, we demonstrate that a subset of GRPR spinal neurons show persistent, cell-intrinsic Ca^{2+} oscillations. These experiments provide the first population-level view of the spinal neurons that respond to pruritic stimuli and pinpoint the output neurons that convey itch to the brain.

Introduction
Itch is an unpleasant sensation that drives organisms to scratch. Itch-inducing stimuli are detected by peripheral sensory neurons that innervate the skin, conveyed to the spinal cord dorsal horn, and finally relayed to the brain where itch can be experienced as a conscious percept. Itch can also be elicited by exogenous application of specific neuropeptides to the spinal cord, including gastrin-releasing peptide (GRP), substance P (SP) and somatostatin[1–9]. These pharmacological findings have implicated several key spinal neuron populations in itch, including excitatory spinal neurons that express either the gastrin releasing peptide receptor (GRPR) or neurokinin-1 receptor (NK1R), as well as inhibitory spinal neurons that express the somatostatin receptor (SSTR). But since these receptors are found in different populations of spinal neurons[10,11], the manner in which diverse neuropeptides elicit itch remains unclear.

A second outstanding question regarding the spinal circuitry that underlies itch is the identity of the spinal output neurons that convey itch input from the spinal cord to the brain. The existence of an itch-specific population of output neurons has been reported[12], but remains controversial, since several other studies have found a broad overlap between spinal output neurons that respond to pruritogens and those that respond to algogens[13–17]. Nevertheless, spinal projection neurons that respond to chemical pruritogens such as histamine are thought to reside within the superficial dorsal horn (primarily lamina I), ascend within the anterolateral tract, and target supraspinal structures including the parabrachial nucleus and the thalamus[13,16,18,19]. At a molecular level, pruriceptive spinal output neurons have been shown to express *Tacr1*, the gene encoding NK1R[19,20], but most spinal output neurons express NK1R[20–22], and thus whether a subset of NK1R spinal output neurons comprise a pathway for itch requires further investigation.

Here we used two-photon (2P) Ca^{2+} imaging to identify a convergent population of spinal neurons that responds to itch-inducing peptides and cutaneous pruritogens. This convergent itch population includes GRPR interneurons, as well as GRPR-expressing spinoparabrachial neurons, providing evidence that specific populations of spinal neurons are involved in conveying itch to the brain. We also find that GRPR spinal neurons display cell intrinsic Ca^{2+} oscillations. In sum, our findings reveal the population-level organization of the spinal processing of itch.

Results

Itch peptides evoke prolonged activity in superficial dorsal horn neurons that parallels scratching behavior
To visualize population-level activity across spinal excitatory neurons in the superficial dorsal horn, we performed 2P Ca^{2+} imaging using an *ex vivo* spinal cord preparation (Figure 1A). We used transgenic mice harboring the *Vglut2-ires-Cre* and *Rosa-lsl-GCaMP6s* (Ai96) alleles to achieve targeted expression of the calcium-sensitive fluorophore GCaMP6s in excitatory

neurons (*Vglut2*^{Cre}*;Rosa*^{GCaMP6s} mice). The red fluorescent dye, DiI, was injected into the lateral parabrachial nucleus (lPBN), allowing us to identify spinal projection neurons (Figures 1B, 1C). In these experiments, we recorded the activity of excitatory interneurons and DiI labeled spinoparabrachial neurons (SPBNs) across five optical planes (ranging from 0 - 75 μm from the surface of the gray matter) to capture the activity of neurons in lamina I and II (Figure 1D).

GRP, somatostatin (or its analog octreotide), and SP are three neuropeptides that cause scratching when delivered intrathecally[1–9]. We therefore sought to visualize the activity of spinal excitatory neurons that is evoked by the application of these itch-inducing peptides. We anticipated that GRP would drive activity in excitatory neurons because GRPR is a G_q-coupled GPCR that is exclusively expressed in a subset of excitatory neurons in the superficial dorsal horn[4,10,23–26]. In response to bath application of GRP we observed activity in ~60% of spinal excitatory neurons in the superficial dorsal horn that lasted for at least 20 minutes (Figures 1F, 1J, S1A). Given its widespread nature, it is likely that this neural activity was due to a combination of GRPR neurons responding directly to GRP as well as neurons that are activated downstream of GRPR neuron activity. Application of octreotide likewise gave rise to prolonged activity, which was observed in ~35% of excitatory neurons (Figures 1G, 1K, S1B). Because the somatostatin receptors (SSTRs) are G_i-coupled and they are exclusively expressed in subsets of inhibitory neurons[11], the observed activity in excitatory neurons is likely indirect, through a mechanism of disinhibition (e.g., downstream activity). In contrast, the application of SP gave rise to activity in ~6% percent of excitatory neurons for only ~ 5 minutes (Figures 1H, 1L, S1C), consistent with the finding that NK1R is rapidly internalized following its activation[27,28]. We then evaluated corresponding activity within SPBNs in response to GRP, octreotide, and SP (Figure 1M). For each peptide, the overall time course of activity in spinal output neurons was broadly similar to the activity observed in excitatory interneurons (Figures 1N, 1O, 1P, S1D-S1F).

Because itch elicits scratching, we next examined whether the duration of activity in spinal excitatory neurons was consistent with the duration of peptide-evoked scratching. Wild-type mice were injected intrathecally with GRP, octreotide, or SP, and scratch bouts were quantified over time (Figure 1Q). As predicted, the activity of superficial dorsal horn neurons observed in 2P Ca^{2+} imaging studies paralleled scratching evoked by each neuropeptide (Figures 1R-T), consistent with the idea that ongoing spinal neuron activity mediates acute itch behaviors.

Itch neuropeptides engage a convergent spinal neuron population defined by GRPR expression

The simplest explanation for the observation that GRP, octreotide, or SP give rise to scratching is that all three of these peptides activate a convergent population of spinal neurons that is involved in mediating itch. Alternatively, each peptide might elicit itch through the activation of independent neuron populations (Figure 2A). To distinguish between these two models, we applied itch-inducing peptides in series to determine whether they activate common subsets of neurons (Figure 2B). GRP and SP were applied in both the presence or absence of TTX to distinguish between direct responders (e.g., those that express the cognate receptor) and downstream responders (e.g., those whose activity is secondary to the response in GRPR neurons or NK1R neurons) (Figure S2A). The activation of SSTR by octreotide, in contrast, only produces activity in downstream (ds) excitatory neurons via disinhibition, which we refer to as SSTR-ds neurons. In these experiments we recorded from >3000 excitatory neurons, 16% (553/3367 neurons) of which were activated by at least one itch-inducing peptide. A variety of response profiles were observed among the recorded neurons, and neurons were categorized based on these responses. (Figure 2C and S2B). Notably, the order of peptide application did not influence the response profiles that we observed, nor did repeated application of peptides cause tachyphylaxis (data not shown).

A preliminary analysis of these response profiles suggested that a large fraction of SSTR-ds were GRPR neurons or neurons that coexpress GRPR and NK1R (GRPR:NK1R neurons). To examine whether this observation could have occurred by chance, we calculated the theoretical overlap if each itch-inducing peptide activated independent populations and compared this with the observed overlap (Figures 2D, 2E). For instance, the theoretical overlap of GRPR:NK1R:SSTR-ds was 0.1%, whereas the observed overlap was 5.6% (Figure 2E). For statistical analysis, we performed a mixed effect log-linear regression to calculate an odds ratio (OR), which reflects whether an observed overlap of populations is larger or smaller than would be expected if the populations were independent. These analyses can be considered an extension of the classic chi-squared test to three or more variables, and further allow us to adjust for differences between mice. We found that the total overlap of GRPR:NK1R:SSTR-ds population was significantly larger than predicted if the populations were independent (Figures 2E and 2F). Dramatic enrichment was also observed in GRPR:NK1R and GRPR-SSTR-ds populations.

These findings suggested that the earliest point of convergence of GRP, SP, and octreotide signaling is on neurons that express both GRPR and NK1R and are downstream of inhibitory SSTR neurons. In light of this, we reasoned that there would be an additional point of convergence: a common population that is downstream of the GRPR:NK1R:SSTR-ds population. To investigate this idea, we performed analogous statistical analyses to ask whether the overlap of GRPR, SSTR, and NK1R downstream neuron populations was greater than that expected by chance. These analyses showed that the populations downstream of GRPR, NK1R, and SSTR neurons overlap extensively, with the greatest enrichment observed within the GRPR-ds:NK1R-ds:STTR-ds population (Figures S2C, S2D). Together, these results indicate that though different itch peptides act on distinct receptors, they engage a common population of spinal neurons to drive itch that is defined by the expression of GRPR, as well as a common population of neurons that is activated downstream of GRPR.

GPRR neurons encode responses to cutaneous pruritogens

Our next goal was to visualize the neurons that are activated by a cutaneous itch stimulus, and to determine whether pruritic input from the periphery activates the same excitatory convergent spinal neuron population as that activated by spinally-applied peptides. To address this question, we used 2P Ca^{2+} imaging of an *ex vivo* somatosensory preparation in which the hairy skin of the dorsal hindpaw through the proximal hip and corresponding nerves (saphenous and lateral femoral cutaneous) were dissected *in continuum* from the skin through the dorsal root ganglia and to the intact spinal cord (Figures 3A, 3B). As in earlier experiments, excitatory neurons were visualized using *Vglut2*^{Cre}*; Rosa*^{GCaMP6s} mice and SPBNs were back labeled with DiI. During imaging sessions, we first mapped the receptive fields of spinal dorsal horn neurons with punctate mechanical stimuli (Figure 3C). As a control stimulus for the mechanical distension of the skin associated with an intradermal injection, saline was delivered into the skin. The activity associated with a saline injection, while robust in those cells whose receptive fields overlapped with the injection sites, lasted between 10 and 20 seconds and was unitary in nature (Figure 3E). Next, the pruritogen compound 48/80, which causes mast cell degranulation and is a model of urticaria[29], was injected intradermally into the skin. After waiting for the compound 48/80 activity to resolve, the itch-inducing peptides GRP and octreotide were then applied to examine whether these agents activated the same network of neurons as compound 48/80. Finally, pharmacological profiling was performed to identify cell types based on receptor-mediated responses.

Compound 48/80 elicited activity in ~35% of all excitatory superficial dorsal horn neurons (Figures 3D, 3E, 3F, S3A). As with application of itch-inducing peptides, the effects of compound 48/80 on spinal neuron activity paralleled the duration of compound 48/80-evoked scratching, which peaks within 5 minutes following injection, and persists for at least 30 minutes (Figures 3G, 3H). We then used our previously characterized pharmacological cell profiling method[30] to assign molecular identities to which spinal neuron populations responded to compound 48/80. The ligands that we used for this profiling allowed us to visualize neurons that express GRPR, NK3R, TRHR, OXTR, CCKR, NK1R, and CHRM3, thereby enabling the identification of 66% of neurons (351/535 compound 48/80-responsive neurons) in lamina I and IIi (Figures 3I, 3J, 3K). While compound 48/80-responsive cells were activated by a variety of ligands (Figure S3B), the ligand that activated the greatest number of compound 48/80 neurons was GRP, suggesting that compound 48/80-responsive neurons include GRPR neurons (Figure 3K). In particular, 31% of the neurons activated by compound 48/80 were GRPR neurons. Because a single neuron can express multiple receptors for these ligands[30], we then evaluated whether specific receptors were associated with whether a neuron responded to cutaneous application of compound 48/80. The receptor that was most strongly associated with activity in response to compound 48/80 was GRPR (Figure 3L, S3C), with 57% of all GRPR neurons responsive to compound 48/80 (185/325 GRPR neurons). Finally, we analyzed which subset of GRPR spinal neurons responded to compound 48/80 and found that they were the GRPR neurons that belong to the convergent itch spinal neuron population (i.e., those that respond to either octreotide and/or SP) (Figures 3M, 3N). In other words, there appears to be a subset of GRPR neurons that are activated by multiple itch-inducing compounds, which we refer to here as GRPR itch neurons. In sum, these analyses show that peripheral pruritic input activates the same excitatory convergent spinal neuron population as that activated by spinally-applied peptides, and identify GRPR itch neurons as the primary excitatory cell-type that responds to compound 48/80.

GRPR spinal projection neurons convey chemical itch to the parabrachial nucleus

We next examined which population(s) of SPBNs are activated in response to the cutaneous injection of compound 48/80. Compound 48/80 elicited prolonged activity in 60% of SPBNs (Figures 4A, 4B, 4C, S4A), of which 96% could be categorized by their responses to agonists used for pharmacological profiling (Figure 4D). Consistent with the idea that NK1R is expressed in the majority of lamina I SPBNs[20–22], SP activated 73% of compound 48/80-responsive SPBNs. Unexpectedly, GRP activated 78% of compound 48/80- responsive SPBNs, suggesting that GRPR is functionally expressed in SPBNs (Figure 4E). Of the compound 48/80-responsive SPBNs that expressed GRPR, nearly all of these were GRPR itch neurons (Figure 4F). In contrast, nearly all SPBNs that were unresponsive to compound 48/80 failed to respond to GRP, and therefore do not express GRPR (Figure 4E). Together, these data show that GRPR SPBNs underlie the transmission of itch input to the brain.

The observation that GRPR is functionally expressed in SPBNs was surprising because previous evidence suggested GRPR is exclusively expressed in spinal interneurons[24,31]. To explore the possibility that GRPR is expressed in spinal output neurons further, we performed fluorescent *in situ* hybridization on wild-type mice in which SPBNs were retrogradely labeled with virus and probed for expression of *Grpr* (Figure 4G). As a positive control, sections were co-stained with *Tacr1*, the gene encoding NK1R, which was detected in 85% of SPBNs (Figures 4H, S4C). *Grpr* was expressed in a subset of spinal output neurons, and the majority (75%) of *Grpr* SPBNs co-expressed *Tacr1* (Figures 4H, S4B, S4C). Consistent with coexpression of GRPR and NK1R at the mRNA level, we analyzed Ca^{2+} responses of SPBNs to GRP and SP in the presence of TTX. Again, we found strong overlap, with 71% of GRPR SPBNs co-expressing NK1R (Figures S4D-S4F). Thus, within the dorsal horn, GRPR expression is not restricted to

excitatory interneurons; rather GRPR is expressed in two distinct populations: excitatory interneurons, as previously described, and spinoparabrachial output neurons.

Lastly, to visualize the central projections of GRPR spinal output neurons, we used *Grpr-Cre* mice and cre-dependent anterograde labeling through viral expression of AAV2-hsyn-DIO-mCherry in the lumbar spinal cord (Figures 4I, 4J). In these mice, we observed ascending fiber tracts within the anterolateral tract on both the contralateral and ipsilateral sides (Figure 4K). Within the brain, the most prominent targets of *Grpr-Cre* spinal output neurons were the lateral parabrachial nuclei, which were labeled on both the contralateral and ipsilateral sides (Figures 4L, 4M) (3 of 3 mice analyzed). In a subset of mice, sparse mCherry^{+} projections were also observed in the the rostral ventral medulla (RVM, 2 of 3 mice) and the caudal ventral posterior thalamus (cVPL, 1 of 3 mice) (Figures 4N, 4O). This projection pattern suggests that GRPR spinal output neurons are a subset of lamina I spinal output neurons that bilaterally collateralize to the parabrachial nucleus.

A subset GRPR spinal neurons display cell-intrinsic Ca^{2+} oscillations

Throughout our Ca^{2+} imaging studies, we noted that GRP elicited a pattern of Ca^{2+} activity in a subset of spinal neurons that was visually distinct. In these cells, the application of GRP for 3 minutes gave rise to repeated Ca^{2+} transients that lasted at least 20 minutes, and in one experiment, at least 80 minutes (Figures 5A, 5B, S5A). To distinguish whether these long-lasting oscillations were a consequence of ongoing network activity, or whether the oscillations were a cell autonomous phenomenon (Figure 5C), we repeated the GRP application in the presence of TTX. This experiment revealed that GRP-induced oscillations occurred for a similar duration even when network activity was silenced, suggesting that GRPR neuron oscillations are cell-intrinsic (Figure 5D, 5E, S5B). To quantify this phenomenon, intrinsic Ca^{2+} oscillations were defined as 3 or more Ca^{2+} transients with similar amplitudes that occurred at regular intervals in response to the brief application of GRP in the presence of TTX (Figure 5F). To determine whether these intrinsic Ca^{2+} oscillations are specific to GRP, we tested the effect of other GPCR agonists (Figure 5G). In addition to GRP, both taltirelin and SP elicited Ca^{2+} oscillations in excitatory neurons in the dorsal horn; however, GRP was more strongly associated with inducing Ca^{2+} oscillations than any other ligand (Figure 5H). Specifically, application of GRP gave rise to persistent Ca^{2+} oscillations in ~30% of GRP-responsive cells. Because a single neuron can express multiple receptors for these GPCR ligands[30], we then evaluated whether specific cell-types were associated with Ca^{2+} oscillations. In the case of SP, neurons that express NK1R were only associated with oscillations if they also expressed GRPR (“GRPR:NK1R”, Figure 5I); a similar trend was observed for neurons that oscillated in response to taltirelin and expressed TRHR (“GRPR:TRHR” Figure 5J). Together, these findings suggest that expression of GRPR is a shared feature of neurons that oscillate, regardless of which agonist causes oscillations.

These findings suggest that a subset of spinal GRPR neurons is notable in their capacity for cell autonomous Ca^{2+} oscillations in response to GRP. The shape and periodicity of these Ca^{2+} oscillations in GRPR neurons were reminiscent of a very well characterized phenomenon involving cycles of IP_3-mediated Ca^{2+} release and SERCA-mediated re-uptake (Figure 6SC)[32–34]. Consistent with this mechanism, we found that GRP-induced Ca^{2+} oscillations were abolished in the presence of the IP_3 receptor antagonist 2-Aminoethoxydiphenyl borate (2-APB) (Figure 5SD) and triggered spontaneously in the presence of the SERCA pump-inhibitor, CPA (Figure S5E). This type of IP_3-mediated Ca^{2+} oscillation has been extensively characterized in a variety of cell types, such as oocytes, pancreatic acinar cells, and osteoclasts[35–37]. Our observations reveal that cell autonomous Ca^{2+} oscillations are also observed in the nervous system, notably in spinal GRPR neurons.

Discussion

In this study, we visualized the itch-responsive neurons in the dorsal horn at the population level for the first time. First, we found that itch-causing agents drive spinal neuron activity that parallels the time course of scratching responses. We then sought to understand how itch is encoded at the population level and found that each itch agent we tested recruited a shared population of spinal interneurons, with expression of GRPR being a defining feature of this itch population. Next, we discovered that GRPR-expressing SPBNs underlie transmission of itch from the spinal cord to the brain. Lastly, we discovered that GRPR neurons show a distinctive property in that they are capable of persistent, cell-intrinsic Ca^{2+} oscillations.

Population coding of itch

Many studies have investigated the contributions of individual cell-types in the dorsal horn to itch, but what has been lacking is a population-level analysis of how itch is encoded. In this study, we addressed this fundamental gap in knowledge through 2P Ca^{2+} imaging of the spinal cord dorsal horn. We asked whether three peptides that elicit robust scratching engage a common population of spinal neurons. We found that octreotide acts through disinhibition to drive activity in a population of excitatory neurons that coexpress GRPR and NK1R. These findings are in keeping with and extend the findings of our recent study demonstrating that NK1R is coexpressed within GRPR neurons and that NK1R spinal neurons play a role in itch[4]. Moreover, our analyses revealed that convergence continues with a common population of neurons downstream of GRPR, NK1R, and SSTR neurons. Thus, our study provides novel insight into the mechanisms by which diverse peptides give rise to itch at the population level. We next visualized the spinal neuron populations activated in response to a cutaneous pruritogen, and found that compound 48/80 recruits the same population of GRPR itch neurons. Together, these data reveal that a common population of neurons underlies scratching that occurs in response to a variety of pruritic agents, both cutaneous and spinal.

GRPR spinal neurons are heterogeneous

GRPR spinal neurons have a well-established role in the spinal transmission of itch[1,3,4,20,38–41]. In studies in which GRPR spinal neurons were neurotoxically ablated, itch behaviors were disrupted, while pain behaviors were spared, leading to the idea that GRPR spinal neurons specifically encode itch[38,41]. Our 2P Ca^{2+} imaging studies underscore that GRPR spinal neurons are central to the population coding of itch, as GRPR expression is the defining feature of neurons that belong to the convergent itch population, and GRPR expression is strongly associated whether excitatory neurons were activated by compound 48/80. However, GRPR spinal neurons were not exclusively found within the convergent itch population, nor did all GRPR neurons respond to injection of compound 48/80, supporting the idea that GRPR neurons are a functionally diverse population of neurons. This is consistent with the idea that GRPR is expressed in several different populations of spinal neurons that may have distinct functions, including itch, noxious heat and mechanical stimuli[25], as well as mechanical allodynia[42]. Heterogeneity of GRPR neurons is further supported by the detection of *Grpr* in several excitatory dorsal neuron cell-types identified in single cell RNA-seq analyses[10,43], as well as their spatial distribution throughout the superficial dorsal horn laminae I-IIo[26,30,31,38]. Thus, we propose that there are at least two functional subtypes of GRPR spinal neurons: one subtype that transmits itch stimuli and belongs to a convergent itch population and another that contributes to transmission of nociceptive stimuli. This framework also extends to NK1R and SSTR neuron populations, which show a broad laminar distribution throughout the superficial dorsal horn[4,44,45], and have been implicated in central sensitization-induced thermal and mechanical hypersensitivity and gating mechanical pain, respectively[46–49]. In sum, we show that

diverse stimuli that drive scratching do so by recruiting a common population of spinal neurons. Whether this neural organization extends to the manifestation of other aspects of somatosensation is an exciting possibility that merits further investigation.

Spinal output neurons for itch

The spinal output neurons that relay itch to the brain have remained largely enigmatic. Chemical itch stimuli have been shown to activate SPBNs that express *Tacr1*[17,19]. However, this classification encompasses the majority of lamina I spinal output neurons[20–22], and thus whether a distinct subset of these neurons represents the output channel of itch to the brain was unknown. Here, we found the vast majority of SPBNs within the superficial dorsal horn that respond to compound 48/80 express GRPR. Consistent with previous studies[19,20], these GRPR spinal projection neurons coexpress NK1R, and we further show these are GRPR itch neurons that are activated by other itch peptides like SP and octreotide. The finding that GRPR neurons are composed of both interneurons and spinal output neurons was surprising, as they have historically been shown to be exclusively interneurons. This idea stems from previous studies in which retrograde labeling of SPBNs failed to label GRPR neurons[24,31]. One possible explanation for the absence of back labeled neurons in these studies is that genetic tools were used to visualize GRPR spinal neurons (rather than direct detection of the receptor), which may have failed to capture the small proportion of GRPR that are spinal output neurons.

After identifying GRPR spinal output neurons through retrograde labeling strategies of the parabrachial nucleus, we then asked whether these neurons represent the subset of SPBNs that collateralize to other brain nuclei[50–52]. Anterograde labeling revealed *Grpr-Cre* neurons predominantly target the contralateral and ipsilateral lPBN. Consistent with this, a previous study using another genetic allele (*Grpr-Cre*^{ERT2}) reported labeling of GRPR spinal neurons in these brain regions[53]. The finding that the spinal projection neurons for chemical itch appear to specifically target the PBN is particularly interesting when put into the context of the spinal output neurons for mechanical itch, which were recently shown to exclusively target the PBN[19]. Taken together, these findings suggest the PBN serves as the initial point of processing of itch input within supraspinal circuits.

An updated model for the spinal coding of itch

In summary, this study provides an updated model of the spinal transmission of itch. In this model, a convergent population of interneurons within the superficial dorsal horn that expresses GRPR integrates itch signals that arise from peripheral stimuli, as well as local spinal neuropeptides. Based on evidence that GRPR interneurons arborize in lamina I and make synaptic contacts onto SPBNs,[25,31,53] we propose GRPR interneurons make direct connections with GRPR SPBNs. While we also identified a convergent neuron population downstream of GRPR interneurons that integrates itch inputs, further studies are required to understand where these neurons fit within a model of spinal itch transmission, though one possibility is that they provide inputs onto GRPR spinal output neurons to further shape the coding of sensory inputs to the parabrachial nucleus. More broadly, in this study we examined how previously defined spinal cell-types are organized at a population level. This approach can be used as a framework in future studies to enable our understanding of the logic of other aspects of spinal somatosensory processing.

Methods

Animals

Animals were cared for in compliance with the National Institutes of Health guidelines and experiments were approved by the University of Pittsburgh Institutional Animal Care and Use Committee. *Vglut2-Cre* (Jax, #016963), *RCL-GCaMP6s* (Jax, #028866), and *Grpr-Cre* (Jax, #036668) mouse lines were obtained from Jackson labs. All transgenic mouse lines were maintained on a C57L7/6 background. C57BL/6 mice were obtained from Charles River (strain 027). All experiments used a combination of male and female mice. Mice were housed in groups of up to four (males) or five (females) under a 12/12 hr light/dark cycle. Cages were lined with wood chip bedding. Food and water were provided *ab libitum*, and plastic housing domes were provided for enrichment.

Viruses

The following viruses were used for anterograde and retrograde labeling of SPBNs: AAV2-hsyn-DIO-mCherry (Addgene, #50459-AAV2), AAV2-hsyn-DIO-hM3Dq-mCherry (Addgene, #44361-AAV2), AAVr-Ef1A-Cre (Addgene, #55636-AAVrg0 titers), and AAVr-hSyn-eGFP-Cre (Addgene, #105540-AAVrg). Viruses were delivered into the spinal cord or parabrachial nucleus undiluted ranging from titers of 8.6×10^{10} to 2.5×10^{13}.

Stereotaxic injection and retrograde labeling of spinoparabrachial neurons

Stereotaxic injections were performed on 3.5-5 week old mice for 2P Ca^{2+} imaging experiments and 7-8 week old mice for fluorescent *in situ* hybridization experiments. Mice were anesthetized with 4% isoflurane and maintained in a surgical plane of anesthesia at 2% isoflurane. They were then head-fixed in a stereotaxic frame (Kopf, model 942) and prepared for surgery: the head was shaved, ophthalmic eye ointment was applied, local antiseptic (betadine and ethanol) was applied, and a scalpel was used to make an incision and expose the skull. The skull was leveled using cranial sutures as landmarks. A drill bit (Stoelting 514551) was used to create a burr hole in the skull and a glass capillary filled with a retrograde tracer was lowered through the hole to the injection site. The parabrachial nucleus was targeted at the following coordinates: AP: -5.11 mm, ML ±1.25 mm, -3.25 mm (from the surface of the skull). A Nanoinject III (Drummond Scientific, 3-000-207) was used to deliver either 250-300 nL of the retrograde tracer Fast DiI oil (2.5 mg/mL) or 500nL of retrograde viruses at 5 nL/s. The glass capillary was left in place for 5 min following the injection and slowly withdrawn. The scalp was sutured closed with 6-0 vicryl suture. For postoperative care, mice were injected with 5 mg/kg ketofen and 0.03 mg/kg buprenorphine and allowed to recover on a heating pad. Experiments began at least 4 days following DiI injection, and at least 5 weeks after viral injection to allow sufficient time for the retrograde label to reach the spinal cord. To verify targeting of retrograde tracers, brains were collected, post-fixed overnight in 4% paraformaldehyde, sunk in sucrose, and sectioned at 60 µm. Sections were checked for fluorescence in the lateral parabrachial nucleus as mapped in the Allen Mouse Brain Atlas.

Ex vivo preparations

Ex vivo preparations for 2P Ca^{2+} imaging were performed on 5-7 week old mice. All solutions were saturated with 95% O_2, 5% CO_2 for the duration of the experiment. Sucrose-based artificial cerebrospinal fluid (aCSF) consisted of (in mM): 234 sucrose, 2.5 KCl, 0.5 $CaCl_2$, 10 $MgSO_4$, 1.25 NaH_2PO_4, 26 $NaHCO_3$, and 11 glucose. Normal aCSF solution consisted of (in mM): 117 NaCl, 3.6 KCl, 2.5 $CaCl_2$, 1.2 $MgCl_2$, 1.2 NaH_2PO_4, 25 $NaHCO_3$, 11 glucose). Mice were anesthetized with ketamine (87.5 mg/kg)/xylazine (12.5 mg/kg) cocktail prior to beginning dissections. Post dissection, the recording chamber was placed in the multiphoton imaging rig and the sucrose-based aCSF was gradually replaced with normal aCSF over 15 min to avoid

shocking the tissue. Meanwhile, the temperature of the aCSF was slowly brought from room temperature to 26°C. Imaging began ~45 min following washout of the recording chamber with aCSF to allow time for recovery of the cells, thermal expansion, and settling of the tissue. Dissection details for each preparation follow below.

Ex vivo spinal cord preparation

Mice were transcardially perfused with chilled, sucrose-based aCSF. The spinal column was dissected out and chilled in sucrose-based aCSF. The ventral surface of the spinal column was removed, and the spinal cord segment corresponding to approximately ranging from the T10 to S1 was carefully removed. Nerve roots were trimmed and the dura and pia mater were removed. Next, using Minutien pins (FST Cat: 26002-202), the spinal cord was secured in a Sylgard-lined recording chamber such that the gray matter of the dorsal horn would be parallel with the imaging objective.

Ex vivo semi-intact somatosensory preparation

The hindpaw, leg, and back were closely shaved, leaving only 2-3 mm of hair in place. Mice were transcardially perfused with chilled, sucrose-based aCSF. An incision was made along the midline of the back and the spinal cord was exposed via dorsal laminectomy. The spinal column, ribs, and leg were excised and transferred to a Sylgard-lined dish and bathed in sucrose-based aCSF. The lateral femoral cutaneous and saphenous nerves were dissected out in continuum from the skin to the dorsal root ganglia. The thoracolumbar spinal cord was carefully removed from the spinal column, keeping spinal roots intact. Next, the spinal cord was securely pinned with Minutien pins as described above and the dura mater was removed along the entire length of the spinal cord. The pia mater was removed from the L1 - L2 recording area. Finally, the nerves and nerve roots were gently loosened from the tissues, and the skin was pinned out as far from the spinal cord as possible, allowing for a light shield to be placed between the skin and objective at the spinal cord during cutaneous injections.

Multiphoton imaging

2P Ca^{2+} imaging was performed on a ThorLabs Bergamo II microscope equipped with an 8 kHz resonant-galvo scanpath, GaAsp detectors, a piezo objective scanner for high-speed Z-control during volumetric imaging, and paired with a Leica20X (NA1.0) water immersion lens. A Spectra Physics Mai Tai Ti:Sapphire femtosecond laser tuned to 940 nm was used to excite the fluorophores. Fluorescence was captured with FITC/TRITC emission filter sets with a 570 nm dichroic beam splitter. Five different planes were imaged simultaneously at 8.5 Hz with 15 µm between planes, providing an imaging depth of 0 - 70 µm below the surface of the gray matter. Scanning was performed with a 1.4x optical zoom at a 512 x 256 pixel resolution providing a 514 x 257 µm field of view, yielding a pixel resolution of 1 µm/pixel. This volumetric scanning approach allowed simultaneous sampling from lamina I and II, and yielded between 250-600 excitatory neurons per experiment.

Receptive field mapping in the *ex vivo* semi-intact somatosensory preparation

In experiments evaluating cutaneous itch inputs, receptive field mapping was performed under low magnification to empirically identify the region of gray matter receiving primary afferent input from the skin as described previously[30]. Briefly, a wide brush was used as a search stimulus to pinpoint the correct field of view. A wide brush was swept over the entire length of dissected skin, activating as many afferent inputs as possible. The imaging region was refined iteratively until the region with the most fluorescence was in the field of view, and the final 1.4x optical zoom was applied. Next, a 2.0 g von Frey filament was applied to the skin in order to locate the 15 x 15 mm region of skin that received the greatest afferent input, which was marked with a

surgical felt tip pen. Imaging, feedback sensors (thermocouples, load cells, etc.), and event times were synchronized using Thosync.

Intradermal injections in the *ex vivo* semi-intact somatosensory preparation

Injection of either saline or compound 48/80 (91 µg in 10 µL) was performed with a fine 31-gauge needle. Saline was randomized to be given either before or after compound 48/80, and no significant differences were noted in the response. The injection site for both compound 48/80 and saline were centered in the area of skin which elicited the largest response to mechanical stimuli. The needle was held nearly parallel with the skin, bevel side up, and carefully inserted into the skin a minimal amount. An injection was considered successful if it resulted in a visible bleb that did not immediately disappear.

Drug applications to *ex vivo* preparations

To measure network-level activity evoked by itch-causing peptides, ligands were bath-applied to the spinal cord. GRP (300 nM) and octreotide (200 nM) were applied for 3 and 7 min, respectively, and subsequent activity was recorded for 20 min. SP (1µM) was applied to the spinal cord for 3 min, and subsequent activity was recorded for 5 min. To determine whether neurons responded directly to itch-causing peptides and GPCR ligands used for pharmacological profiling, 500 nM TTX (Abcam 120055) was applied to the spinal cord and allowed to circulate for 8-15 min to suppress network activity. Then, agonists were diluted in TTX and applied to the spinal cord for 3 min at the following concentrations: GRP, 300 nM (Tocris 1789); SP, 1 µM (Sigma S6883); NKB, 500 nM (Tocris 1582); taltirelin, 3 µM (Adooq Bioscience A18250); oxytocin, 1µM (Sigma O4375); CCK, 200 nM (Tocris 11661); oxotremorine M, 50 µM (Tocris 1067). The tissue was washed with aCSF with TTX for 5 min between ligand applications. At the end of each experiment, a 30 mM KCl was applied for ~ 45 sec to confirm cell viability.

Image processing and data extraction

Recording files were prepared for image processing using macros in FIJI (Image J, NIH). Macros are available on github (https://github.com/cawarwick/ThorStackSplitter). Suite2p (HHMI Janelia) was used for image registration. Then, another ImageJ macro (https://github.com/cawarwick/Suite2p-Output-Processor) was used to review stabilized recordings, generate summary images ROI for selection, and produce averages of the recordings to assist in refining ROIs. We preferred manually selecting ROIs as opposed to using suite2p generated masks because of the heterogeneity of spinal neurons soma size left SPBNs undetected by suite2p. Only cells that had a stable XY location and were free of Z drift were included in analyses. Following ROI selection, FIJI was used to extract raw mean fluorescence intensity. Using either R or Python (Full Python analysis pipeline available on guthub: https://github.com/AbbyCui/CalciumImagingAnalysis), the ΔF/F for each neuron ROI was calculated using the following rolling ball baseline calculation: for each frame (F_i) the 20th percentile value of the surrounding 6.6 min of frames was used as a baseline (F_b) to perform the ΔF/F calculation ($(F_i-F_b)/F_b$). Rolling ball normalization was applied to minimize effects of gradual photobleaching of GCaMP6s and/or minor changes in ROI location. ΔF/F values for each cell then were plotted over time and traces were visually reviewed. ROIs with recordings that demonstrated Z-drift, were unresponsive to KCl application, or exhibited cell death over the course of the recording were omitted from analysis. Neurons demonstrating basal spontaneous activity were included in counts of total neurons recorded, but were uninterpretable and thus excluded from analyses for responsiveness to itch-inducing neuropeptides or cutaneous stimuli.

Analysis of Ca^{2+} activity

For analyses of ongoing neuronal activity in response to itch-inducing peptides and compound 48/80, the area under the curve (AUC) of Ca^{2+} activity was calculated for each cell. To determine a response threshold, we first manually identified cells with a visually robust, sustained Ca^{2+} response from a dataset of ~750 neurons. A receiver operator characteristic analysis was then performed, and the AUC value with 95% specificity was selected to minimize inclusion of false positives. The average AUC threshold was determined by dividing the cumulative AUC threshold by the number of 2.5 min bins (GRP, octreotide, compound 48/80) or 1 min bins (SP) in the recording. This corresponded to an average AUC of at least (0.462 Seconds*ΔF/F)/bin relative to baseline activity. If cells met this AUC threshold, they were labeled as responders for a given stimulus. For analyses categorizing neurons for convergent population analyses as well as responses to GPCR agonists, neurons were classified as binary responders (yes/no). Neurons were considered binary responders if they displayed a peak Ca^{2+} response within 60 s of applying pharmacological stimuli with an increase in ΔF/F that was both ≥ 30% and ≥ 5 SDs of baseline activity in the 30 s preceding stimulus application. The response window was chosen to account for variability in time required for different drugs to penetrate the spinal cord and their subsequent activation of intracellular signaling cascades.

Behavior

All behavior experiments were conducted on mice from a C57BL/6J background. Behavior was conducted in a designated, temperature controlled room, with an experimenter blinded to treatment in order to minimize bias. Injection sites were shaved at least 24 hr prior to testing. On the day of testing, mice were allotted 30 min to acclimate to a plexiglas chamber on an elevated platform. Behavior platforms had a translucent glass surface, enabling bottom-up recording of animals using a Sony HD Camera (HDR-CX405). The experimenter left the behavior room once the last animal was injected. Only mice that were successfully injected were included in data analysis. Behavior was later scored by an observer blind to treatment. All behavior experiments were performed during the light cycle between 9 A.M. and 6 P.M.

Intrathecal neuropeptide-evoked scratching

Itch peptides were administered intrathecally to awake, behaving mice. Mice were pinned by their pelvic girdle and a 25-μL Hamilton Syringe with a 30-G needle attachment was inserted between the L5 and L6 vertebrae. Successful targeting of the intervertebral space was demonstrated by a sudden involuntary lateral tail movement. A total of 5 *μ*L of drug was injected at a rate of 1 μL/s, and the needle was held in place for 5 s prior to removal to minimize backflow. The following peptides were delivered in 5μL of sterile saline: GRP (295 ng, Tocris 1789), Substance P (400 ng, Sigma S6883), octreotide (30 ng, Tocris 1818), GR 73632 (40 ng, Tocris 1669). Following injection, mice were returned to their plexiglas behavior chambers and recorded for 5-20 min.

Intradermal pruritogen-evoked scratching

A 25-μL Hamilton Syringe with a 30-G needle attachment was used to deliver compound 48/80 (91 μg in 10uL, Sigma C2313) intradermally in the nape of the neck. A successful intradermal injection was indicated by the appearance of a bleb at the injection site. Following injection, mice were returned to their plexiglas behavior chambers and recorded for 30 min.

RNAscope fluorescent *in situ* hybridization (FISH)

Animals were anesthetized with isoflurane and quickly decapitated. The L3-L5 spinal cord segments were rapidly removed, flash frozen, and 15 μm sections were directly mounted onto Superfrost Plus slides. FISH experiments were performed according to manufacturer's

instructions for fresh frozen samples (Advanced Cell Diagnostics, 320293 or 323100). Briefly, spinal cord sections were fixed in ice-cold 4% paraformaldehyde for 15 min, dehydrated in ethanol, permeabilized at room temperature with protease for 15 min, and hybridized at 40°C *w*ith gene-specific probes to mouse, including: *Grpr* (#317871), *Tacr1* (#428781), *Cre* (#474001), *Tac1* (#410351), *Grp* (#317861). Hybridized probe signal was then amplified and fluorescently labeled. Slides were mounted with Prolong Gold with DAPI to visualize nuclei.

Intraspinal injections

Intraspinal viral injections were performed on 5-7 week old mice. Animals were anesthetized with a ketamine (95 mg/kg)/xylazine(4.8 mg/kg)/acepromazine cocktail (0.95 mg/kg). They were then prepared for surgery: the back was shaved, local antiseptic (betadine and ethanol) was applied to the skin, and a scalpel was used to make an incision over the T12-L3 vertebrae. Muscle and fascia were removed, exposing the L3/L4 and L4/L5 spinal segments. For each segment, a glass capillary filled with virus was lowered 300 µm below the surface of the spinal cord to target the dorsal horn, and a Nanoinject III was used to deliver 500 nL of virus at 5 nL/s. The glass capillary was left in place for 5 min following each injection and slowly withdrawn. The skin was sutured closed with 6-0 vicryl suture. For postoperative care, mice were injected with 5 mg/kg ketofen and 0.03 mg/kg buprenorphine and allowed to recover on a heating pad. Histology experiments began at least 4 weeks following viral injection to allow sufficient time for the viral labeling to reach the brain.

Immunohistochemistry

For histology studies visualizing the central projection of spinal output neurons, mice were anesthetized with intraperitoneal injection urethane (4 mg/kg, i.p.) and transcardially perfused with 4% paraformaldehyde. Spinal cord and brain were removed and post-fixed in 4% paraformaldehyde for either 2 hr (spinal cord) or overnight (brain). Tissues were then washed in PBS with 0.3% triton (PBS-T), sunk in 30% sucrose, and cryosectioned at either 20 µm (spinal cord) or 40 µm (brain). Sections were incubated in a blocking solution made of 10% donkey serum (Jackson ImmunoResearch, 017-000-121) and 0.3% triton in PBS for 1 hr at room temperature. Sections were incubated overnight at 4°C with the primary antibody rabbit anti-RFP (Rockland, 600-401-379) diluted at 1:1K in an antibody buffer consisting of 5% donkey serum and 0.3% triton in PBS. Following washes in PBS-T, sections were incubated for 1 hr at room temperature with the secondary antibody donkey anti-rabbit Alexa Fluor 555 (Invitrogen, A-31572) at 1:500 diluted in antibody buffer. Tissues were washed in PBS and mounted with Prolong Gold with DAPI (Invitrogen, P36931).

Image acquisition and quantification

Full-thickness tissue sections were imaged using an upright epifluorescent microscope (Olympus BX53 with UPlanSApo 4x, 10x or 20x objective) or confocal microscope (Nikon A1R with an 20x oil-immersion objective). Image analysis was performed off-line using FIJI imaging software (Image J, NIH). In FISH experiments evaluating markers in superficial dorsal horn neurons, the superficial dorsal horn was defined as the region between the surface of the gray matter and the bottom of the substantia gelatinosa, a region ~ 65 µm thick corresponding to lamina I and II. For FISH experiments visualizing retrogradely labeled SPBNs, 9-15 hemisections per mouse were imaged to ensure enough sparsely labeled projection neurons were available for analysis. In immunohistochemistry experiments assessing the central targets of *Grpr-Cre* spinal projection neurons, brain sections from 3 mice were imaged and brain structures with mCherry signal were recorded.

Quantification and statistical analysis

Microsoft Excel, GraphPad Prism, EulerAPE[54], R, and Python packages including Scipy, numpy, pandas, matplotlib, and other custom code were used for data organization, processing, visualization, and statistical analyses. Log-linear analyses were used to test whether populations of neurons overlap more than expected by chance. Differences between mice were adjusted for using a mixed-effect model (i.e., a random intercept for mouse) when data were available for at least six mice. Otherwise, models included fixed-effects to adjust for the effect of each mouse. Analyses of neuronal responses to GPCR agonists were run as logistic (i.e., binary outcome) and linear (AUC) regressions, adjusting for mouse as fixed-effects. Throughout the figures, statistical significance is indicated with the following symbols: *$p < 0.05$, **$p < 0.01$, ***$p < 0.001$, ****$p < 0.0001$, ^^^$p < 1 \times 10^{-8}$, ^^^^$p < 1 \times 10^{-8}$. A Bonferroni correction was used to correct for multiple comparisons, when appropriate. Experiment-specific details can be found in the figure legends. Data are presented as mean ± SEM, with a few exceptions. Odds ratio analyses are presented as the odds ratio estimate ± upper and lower 95% CI. Linear regression analyses are presented as estimate ± upper and lower 95% CI.

Key Resources Table		
REAGENT or RESOURCE	**SOURCE**	**IDENTIFIER**
Antibodies		
rabbit α-RFP	Rockland	Cat#600-401-379; RRID: AB_2209751
donkey α-rabbit Alexa Fluor 555	Invitrogen	Cat#A-31572; RRID: AB_162543
Bacterial and virus strains		
AAV2-hSyn-DIO-mCherry	Addgene	50459-AAV2
AAV2-hSyn-DIO-hM3Dq-mCherry	Addgene	44361-AAV2
AAVr-Ef1A-Cre	Addgene	55636-AAVrg
AAVr.hSyn.HI.eGFP-Cre.WPRE.SV40	Addgene	105540-AAVrg
Chemicals, peptides, and recombinant proteins		
Compound 48/80	Sigma-Aldrich	Cat#C2313; CAS: 848035-21-2
Chloroquine Diphosphate Salt	Sigma-Aldrich	Cat#C6628; CAS: 50-63-5
FAST DiI™ oil	Invitrogen	Cat#D3899
Octreotide	Tocris Bioscience	Cat#1818; CAS: 83150-76-9
GRP	Tocris Bioscience	Cat#1789; CAS: 93755-85-2
Substance P	Sigma-Aldrich	S6883; CAS: 137348-11-9
Taltirelin (Talt)	Adooq Bioscience	Cat#A18250; CAS: 103300-74-9
Oxytocin (Oxy)	Sigma-Aldrich	O4375; CAS: 50-56-6
Oxotremorine (Oxo)	Tocris Bioscience	Cat#1067; CAS: 3854-04-4
Cholecystokinin Octapeptide, sulfated (CCK)	Tocris Bioscience	Cat#11661
Neurokinin B (NKB)	Tocris Bioscience	Cat#1908; CAS: 87096-84-2
Tetrodotoxin citrate (TTX)	Abcam	Cat#ab120055; CAS: 18660-81-6
2-Aminoethoxydiphenyl borate (2-APB)	Tocris Bioscience	Cat#1224; CAS: 524-95-8
Cyclopiazonic acid (CPA)	Tocris Bioscience	Cat#1235; CAS: 18172-33-3
GR, 73632	Tocris Bioscience	Cat#1669; CAS: 133156-06-6
Critical commercial assays		
RNAscope™ Probe- Mm-Grpr	ACDbio	Cat#317871
RNAscope™ Probe- Mm-Tacr1	ACDbio	Cat#428781
RNAscope™ Probe- Cre	ACDbio	Cat#474001
RNAscope™ Probe- Mm-Slc17a6	ACDbio	Cat#456751
RNAscope™ Probe- Mm-Tac1	ACDbio	Cat#410351
RNAscope™ Probe- Mm-Grp	ACDbio	Cat#317861
RNAscope™ Probe- EGFP	ACDbio	Cat#400281
Experimental models: Organisms/strains		
Mouse: *C57BL6/J*	Charles River	Cat: 027
Mouse: *Vglut2-Cre*	Vong et al.[55]	Jax Stock # 016963;
Mouse: *Ai96 (RCL-GCaMP6s)*	Madisen et al. [56]	Jax Stock # 028866
Mouse: *Grpr-Cre*	Munanairi et al.[57]	Jax Stock # 036668
Software and algorithms		

PRISM 9.0	GraphPad	https://www.graphpad.com/scientific-software/prism/
FIJI	ImageJ	https://www.nature.com/articles/nmeth.2019
suite2p	v0.10.0, HHMI Janelia	https://www.suite2p.org/
R	R Core Team (2021)[58]	https://www.r-project.org/
Python	Python 3.10.7	https://www.python.org/
EulerAPE	Micallef and Rodgers[54]	https://www.eulerdiagrams.org/eulerAPE/

Funding

This work was supported by F32NS110155 (TDS), K99NS126569 (TDS), R01AR063772 (SER), R01NS096705 (HRK/SER), RM1NS128775 (HRK).

Acknowledgements

We thank all members of the Ross lab for their comments and suggestions, as well as Michael C. Chiang and Haichao C. Chen for their technical assistance. Select figure panels were created using icons from BioRender.

Declaration of interests

The authors have no competing interests.

Author Contributions

Conceptualization: TDS, SER; Data curation: TDS, CAW, AYC, DAAB. Formal analysis: TDS, CAW, AYC, DAAB. Funding acquisition: TDS, HRK, SER. Investigation: TDS, CAW, AYC, VJP, KMS, EKN, APM. Project administration: TDS. Software: CAW, AYC, DAAB. Supervision: TDS, SER. Visualization: TDS, CAW, AYC. Writing, original draft: TDS. Writing, review and editing: All authors.

References

1. Sun, Y.G., and Chen, Z.F. (2007). A gastrin-releasing peptide receptor mediates the itch sensation in the spinal cord. Nature *448*, 700–703. 10.1038/nature06029.
2. Kardon, A.P., Polgár, E., Hachisuka, J., Snyder, L.M., Cameron, D., Savage, S., Cai, X., Karnup, S., Fan, C.R., Hemenway, G.M., et al. (2014). Dynorphin Acts as a Neuromodulator to Inhibit Itch in the Dorsal Horn of the Spinal Cord. Neuron *82*, 573–586. 10.1016/j.neuron.2014.02.046.
3. Sukhtankar, D.D., and Ko, M.-C. (2013). Physiological Function of Gastrin-Releasing Peptide and Neuromedin B Receptors in Regulating Itch Scratching Behavior in the Spinal Cord of Mice. PLOS ONE *8*, e67422. 10.1371/journal.pone.0067422.
4. Sheahan, T.D., Warwick, C.A., Fanien, L.G., and Ross, S.E. (2020). The neurokinin-1 receptor is expressed with gastrin-releasing peptide receptor in spinal interneurons and modulates itch. J. Neurosci. *40*, 8816–8830. 10.1523/JNEUROSCI.1832-20.2020.
5. Huang, J., Polgár, E., Solinski, H.J., Mishra, S.K., Tseng, P., Iwagaki, N., Boyle, K.A., Dickie, A.C., Kriegbaum, M.C., Wildner, H., et al. (2018). Circuit dissection of the role of somatostatin in itch and pain. 10.1038/s41593-018-0119-z.
6. Ruzza, C., Rizzi, A., Malfacini, D., Cerlesi, M.C., Ferrari, F., Marzola, E., Ambrosio, C., Gro, C., Severo, S., Costa, T., et al. (2014). Pharmacological characterization of tachykinin tetrabranched derivatives. Br. J. Pharmacol. *171*, 4125–4137. 10.1111/bph.12727.
7. Hylden, J.L.K., and Wilcox, G.L. (1981). Intrathecal substance P elicits a caudally-directed biting and scratching behavior in mice. Brain Res. *217*, 212–215. 10.1016/0006-8993(81)90203-1.
8. Gamse, R., and Saria, A. (1986). Nociceptive behavior after intrathecal injections of substance P, neurokinin A and calcitonin gene-related peptide in mice. Neurosci. Lett. *70*, 143–147. 10.1016/0304-3940(86)90453-2.
9. Seybold, V.S., Hylden, J.L.K., and Wilcox, G.L. (1982). Intrathecal substance P and somatostatin in rats: Behaviors indicative of sensation. Peptides *3*, 49–54. 10.1016/0196-9781(82)90141-3.
10. Häring, M., Zeisel, A., Hochgerner, H., Rinwa, P., Jakobsson, J.E.T., Lönnerberg, P., La Manno, G., Sharma, N., Borgius, L., Kiehn, O., et al. (2018). Neuronal atlas of the dorsal horn defines its architecture and links sensory input to transcriptional cell types. Nat. Neurosci., 1. 10.1038/s41593-018-0141-1.
11. Todd, A.J., Spike, R.C., and Polgár, E. (1998). A quantitative study of neurons which express neurokinin-1 or somatostatin sst2a receptor in rat spinal dorsal horn. Neuroscience *85*, 459–473. 10.1016/S0306-4522(97)00669-6.
12. Andrew, D., and Craig, A.D. (2001). Spinothalamic lamina I neurones selectively responsive to cutaneous warming in cats. J. Physiol. *537*, 489–495. 10.1111/j.1469-7793.2001.00489.x.
13. Jansen, N.A., and Giesler, G.J. (2015). Response characteristics of pruriceptive and nociceptive trigeminoparabrachial tract neurons in the rat. J. Neurophysiol. *113*, 58–70. 10.1152/jn.00596.2014.
14. Davidson, S., Zhang, X., Yoon, C.H., Khasabov, S.G., Simone, D.A., and Giesler, G.J. (2007). The Itch-Producing Agents Histamine and Cowhage Activate Separate Populations of Primate Spinothalamic Tract Neurons. J. Neurosci. *27*, 10007–10014. 10.1523/JNEUROSCI.2862-07.2007.
15. Davidson, S., Zhang, X., Khasabov, S.G., Moser, H.R., Honda, C.N., Simone, D.A., and Giesler, G.J. (2012). Pruriceptive spinothalamic tract neurons: physiological properties and projection targets in the primate. J. Neurophysiol. *108*, 1711–1723. 10.1152/jn.00206.2012.
16. Akiyama, T., Curtis, E., Nguyen, T., Carstens, M.I., and Carstens, E. (2016). Anatomical evidence of pruriceptive trigeminothalamic and trigeminoparabrachial projection neurons in mice. J. Comp. Neurol. *524*, 244–256. 10.1002/cne.23839.

17. Wercberger, R., Braz, J.M., Weinrich, J.A., and Basbaum, A.I. (2021). Pain and itch processing by subpopulations of molecularly diverse spinal and trigeminal projection neurons. Proc. Natl. Acad. Sci. U. S. A. *118*, e2105732118. 10.1073/pnas.2105732118.
18. Moser, H.R., and Giesler, G.J. (2014). Characterization of pruriceptive trigeminothalamic tract neurons in rats. J. Neurophysiol. *111*, 1574–1589. 10.1152/jn.00668.2013.
19. Ren, X., Liu, S., Virlogeux, A., Kang, S.J., Brusch, J., Liu, Y., Dymecki, S.M., Han, S., Goulding, M., and Acton, D. (2023). Identification of an essential spinoparabrachial pathway for mechanical itch. Neuron *111*, 1812-1829.e6. 10.1016/j.neuron.2023.03.013.
20. Akiyama, T., Nguyen, T., Curtis, E., Nishida, K., Devireddy, J., Delahanty, J., Carstens, M.I., and Carstens, E. (2015). A central role for spinal dorsal horn neurons that express neurokinin-1 receptors in chronic itch. Pain *156*, 1240–1246. 10.1097/j.pain.0000000000000172.
21. Cameron, D., Polgar, E., Gutierrez-Mecinas, M., Gomez-Lima, M., Watanabe, M., and Todd, A.J. (2015). The organisation of spinoparabrachial neurons in the mouse. Pain *156*, 2061–2071. 10.1097/j.pain.0000000000000270.
22. Choi, S., Hachisuka, J., Brett, M.A., Magee, A., Omori, Y., Iqbal, N., Zhang, D., Delisle, M.M., Wolfson, R.L., Bai, L., et al. (2020). Parallel ascending spinal pathways for affective touch and pain. Nature. 10.1038/s41586-020-2860-1.
23. Zhao, Z.Q., Wan, L., Liu, X.Y., Huo, F.Q., Li, H., Barry, D.M., Kim, S., Liu, Z.C., Chen, Z.F., Zhao, Z.Q., et al. (2014). Cross-inhibition of NMBR and GRPR signaling maintains normal histaminergic itch transmission. J. Neurosci. *34*, 12402–12414. 10.1523/JNEUROSCI.1709-14.2014.
24. Aresh, B., Freitag, F.B., Perry, S., Blümel, E., Lau, J., Franck, M.C.M., and Lagerström, M.C. (2017). Spinal cord interneurons expressing the gastrin-releasing peptide receptor convey itch through VGLUT2-mediated signaling. Pain *158*, 945–961. 10.1097/j.pain.0000000000000861.
25. Polgár, E., Dickie, A.C., Gutierrez-Mecinas, M., Bell, A.M., Boyle, K.A., Quillet, R., Ab Rashid, E., Clark, R.A., German, M.T., Watanabe, M., et al. (2023). Grpr expression defines a population of superficial dorsal horn vertical cells that have a role in both itch and pain. Pain *164*, 149–170. 10.1097/j.pain.0000000000002677.
26. Freitag, F.B., Ahemaiti, A., Jakobsson, J.E.T., Weman, H.M., and Lagerström, M.C. (2019). Spinal gastrin releasing peptide receptor expressing interneurons are controlled by local phasic and tonic inhibition. Sci. Rep. *9*, 1–14. 10.1038/s41598-019-52642-3.
27. Mantyh, P.W., Demaster, E., Malhotra, A., Ghilardi, J.R., Scott, D., Mantyh, C.R., Liu, H., Basbaum, A.I., Vigna, S.R., John, E., et al. (1995). Receptor Endocytosis and Dendrite Reshaping in Spinal Neurons After Somatosensory Stimulation. Science *268*, 1629–1632.
28. Wang, X., and Marvizán, J.C.G. (2002). Time-course of the internalization and recycling of neurokinin 1 receptors in rat dorsal horn neurons. Brain Res. *944*, 239–247. 10.1016/S0006-8993(02)02918-9.
29. Solley, G.O., Gleich, G.J., Jordon, R.E., and Schroeter, A.L. (1976). The late phase of the immediate wheal and flare skin reaction. Its dependence upon IgE antibodies. J. Clin. Invest. *58*, 408–420. 10.1172/JCI108485.
30. Warwick, C., Salsovic, J., Hachisuka, J., Smith, K.M., Sheahan, T.D., Chen, H., Ibinson, J., Koerber, H.R., and Ross, S.E. (2022). Cell type-specific calcium imaging of central sensitization in mouse dorsal horn. Nat. Commun. *13*, 5199. 10.1038/s41467-022-32608-2.
31. Bardoni, R., Shen, K.F., Li, H., Jeffry, J., Barry, D.M., Comitato, A., Li, Y.Q., and Chen, Z.F. (2019). Pain Inhibits GRPR Neurons via GABAergic Signaling in the Spinal Cord. Sci. Rep. *9*, 1–11. 10.1038/s41598-019-52316-0.
32. Sanders, J.R., Ashley, B., Moon, A., Woolley, T.E., and Swann, K. (2018). PLCζ Induced Ca2+ Oscillations in Mouse Eggs Involve a Positive Feedback Cycle of Ca2+ Induced InsP3 Formation From Cytoplasmic PIP2. Front. Cell Dev. Biol. *6*.

33. Nomikos, M., Kashir, J., Swann, K., and Lai, F.A. (2013). Sperm PLCζ: from structure to Ca2+ oscillations, egg activation and therapeutic potential. FEBS Lett. *587*, 3609–3616. 10.1016/j.febslet.2013.10.008.
34. Thul, R. (2014). Translating Intracellular Calcium Signaling into Models. Cold Spring Harb. Protoc. *2014*, pdb.top066266. 10.1101/pdb.top066266.
35. Oikawa, T., Kuroda, Y., and Matsuo, K. (2013). Regulation of osteoclasts by membrane-derived lipid mediators. Cell. Mol. Life Sci. *70*, 3341–3353. 10.1007/s00018-012-1238-4.
36. Zhang, S., Fritz, N., Ibarra, C., and Uhlén, P. (2011). Inositol 1,4,5-Trisphosphate Receptor Subtype-Specific Regulation of Calcium Oscillations. Neurochem. Res. *36*, 1175–1185. 10.1007/s11064-011-0457-7.
37. Matsu-ura, T., Shirakawa, H., Suzuki, K.G.N., Miyamoto, A., Sugiura, K., Michikawa, T., Kusumi, A., and Mikoshiba, K. (2019). Dual-FRET imaging of IP3 and Ca2+ revealed Ca2+-induced IP3 production maintains long lasting Ca2+ oscillations in fertilized mouse eggs. Sci. Rep. *9*, 4829. 10.1038/s41598-019-40931-w.
38. Sun, Y.G., Zhao, Z.Q., Meng, X.L., Yin, J., Liu, X.Y., and Chen, Z.F. (2009). Cellular basis of itch sensation. Science *325*, 1531–1534. 10.1126/science.1174868.
39. Acton, D., Ren, X., Di Costanzo, S., Dalet, A., Bourane, S., Bertocchi, I., Eva, C., and Goulding, M. (2019). Spinal Neuropeptide Y1 Receptor-Expressing Neurons Form an Essential Excitatory Pathway for Mechanical Itch. Cell Rep. *28*, 625-639.e6. 10.1016/j.celrep.2019.06.033.
40. Pagani, M., Albisetti, G.W., Sivakumar, N., Wildner, H., Santello, M., Johannssen, H.C., and Zeilhofer, H.U. (2019). How Gastrin-Releasing Peptide Opens the Spinal Gate for Itch. Neuron *103*, 102-117.e5. 10.1016/j.neuron.2019.04.022.
41. Albisetti, G.W., Pagani, M., Platonova, E., Hösli, L., Johannssen, H.C., Fritschy, J.-M., Wildner, H., and Zeilhofer, H.U. (2019). Dorsal Horn Gastrin-Releasing Peptide Expressing Neurons Transmit Spinal Itch But Not Pain Signals. J. Neurosci. Off. J. Soc. Neurosci. *39*, 2238–2250. 10.1523/JNEUROSCI.2559-18.2019.
42. Noh, M. chul, Corrigan, K.A., Williams, S.P.G., Peirs, C., Zhao, X., Santos, D., Taylor, B.K., and Seal, R.P. (2023). An unexpected player in the circuitry for mechanical allodynia revealed through studies of diabetic neuropathy. In.
43. Russ, D.E., Cross, R.B.P., Li, L., Koch, S.C., Matson, K.J.E., Yadav, A., Alkaslasi, M.R., Lee, D.I., Le Pichon, C.E., Menon, V., et al. (2021). A harmonized atlas of mouse spinal cord cell types and their spatial organization. Nat. Commun. *12*, 5722. 10.1038/s41467-021-25125-1.
44. Shi, T.-J.S., Xiang, Q., Zhang, M.-D., Barde, S., Kai-Larsen, Y., Fried, K., Josephson, A., Glück, L., Deyev, S.M., Zvyagin, A.V., et al. (2014). Somatostatin and its 2A receptor in dorsal root ganglia and dorsal horn of mouse and human: expression, trafficking and possible role in pain. Mol. Pain *10*, 12. 10.1186/1744-8069-10-12.
45. Polgár, E., Durrieux, C., Hughes, D.I., and Todd, A.J. (2013). A Quantitative Study of Inhibitory Interneurons in Laminae I-III of the Mouse Spinal Dorsal Horn. PLoS ONE *8*. 10.1371/journal.pone.0078309.
46. Nichols, M.L., Allen, B., Rogers, S., Ghilardi, J.R., Honore, P., Luger, N.M., Finke, M.P., Li, J., Lappi, D.A., Simone, D.A., et al. (1999). Transmission of Chronic Nociception by Spinal Neurons Expressing the Substance P Receptor. Science, 1558–1562. 10.1126/science.286.5444.1558.
47. Mantyh, P.W., Mantyh, P.W., Rogers, S.D., Honore, P., Allen, B.J., Ghilardi, J.R., Li, J., Daughters, R.S., Lappi, D.A., Wiley, R.G., et al. (1997). Inhibition of Hyperalgesia by Ablation of Lamina I Spinal Neurons Expressing the Substance P Receptor. Science *278*, 275–280. 10.1126/science.278.5336.275.
48. Barik, A., Sathyamurthy, A., Thompson, J., Seltzer, M., Levine, A., and Chesler, A. (2021). A spinoparabrachial circuit defined by Tacr1 expression drives pain. eLife *10*,

e61135. 10.7554/eLife.61135.

49. Duan, B., Cheng, L., Bourane, S., Britz, O., Padilla, C., Garcia-Campmany, L., Krashes, M., Knowlton, W., Velasquez, T., Ren, X., et al. (2014). Identification of spinal circuits transmitting and gating mechanical pain. Cell *159*, 1417–1432. 10.1016/j.cell.2014.11.003.
50. McMahon, S.B., and Wall, P.D. (1985). Electrophysiological mapping of brainstem projections of spinal cord lamina I cells in the rat. Brain Res. *333*, 19–26. 10.1016/0006-8993(85)90119-2.
51. Spike, R.C., Puskár, Z., Andrew, D., and Todd, A.J. (2003). A quantitative and morphological study of projection neurons in lamina I of the rat lumbar spinal cord. Eur. J. Neurosci. *18*, 2433–2448. 10.1046/j.1460-9568.2003.02981.x.
52. Al-Khater, K.M., and Todd, A.J. (2009). Collateral projections of neurons in laminae I, III, and IV of rat spinal cord to thalamus, periaqueductal gray matter, and lateral parabrachial area. J. Comp. Neurol. *515*, 629–646. 10.1002/cne.22081.
53. Mu, D., Deng, J., Liu, K.-F., Wu, Z.-Y., Shi, Y.-F., Guo, W.-M., Mao, Q.-Q., Liu, X.-J., Li, H., and Sun, Y.-G. (2017). A central neural circuit for itch sensation. Science *357*, 695–699. 10.1126/science.aaf4918.
54. eulerAPE: Drawing Area-Proportional 3-Venn Diagrams Using Ellipses | PLOS ONE https://journals.plos.org/plosone/article?id=10.1371/journal.pone.0101717.
55. Vong, L., Ye, C., Yang, Z., Choi, B., Chua, S., and Lowell, B.B. (2011). Leptin Action on GABAergic Neurons Prevents Obesity and Reduces Inhibitory Tone to POMC Neurons. Neuron *71*, 142–154. 10.1016/j.neuron.2011.05.028.
56. Madisen, L., Garner, A.R., Shimaoka, D., Chuong, A.S., Klapoetke, N.C., Li, L., van der Bourg, A., Niino, Y., Egolf, L., Monetti, C., et al. (2015). Transgenic Mice for Intersectional Targeting of Neural Sensors and Effectors with High Specificity and Performance. Neuron *85*, 942–958. 10.1016/j.neuron.2015.02.022.
57. Munanairi, A., Liu, X.-Y., Barry, D.M., Yang, Q., Yin, J.-B., Jin, H., Li, H., Meng, Q.-T., Peng, J.-H., Wu, Z.-Y., et al. (2018). Non-canonical Opioid Signaling Inhibits Itch Transmission in the Spinal Cord of Mice. Cell Rep. *23*, 866–877. 10.1016/J.CELREP.2018.03.087.
58. Team, R.C. (2017). R: A language and environment for statistical computing.

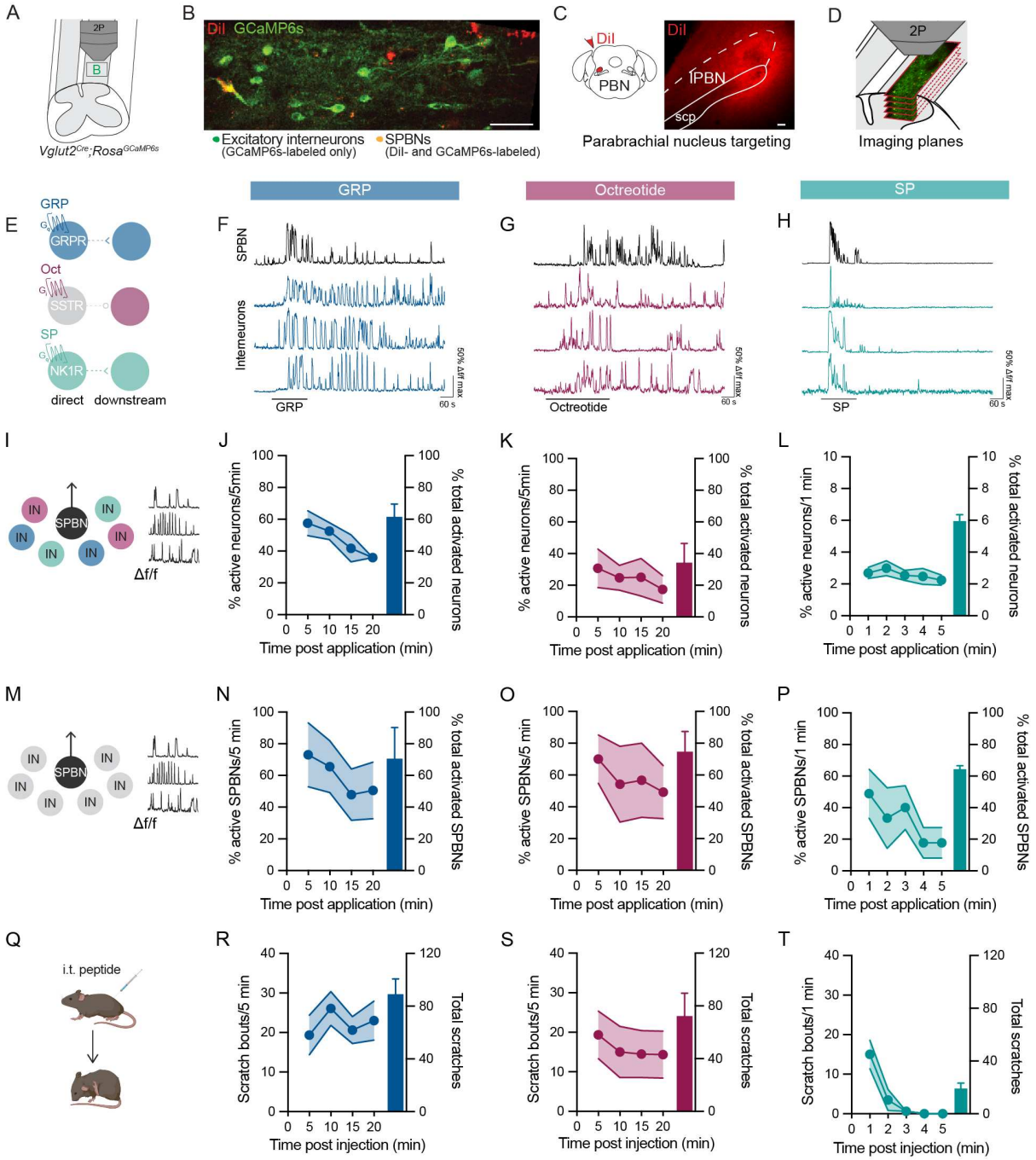

Figure 1. Neuropeptides evoke prolonged activity in spinal neurons that parallels itch behavior

A) 2P Ca^{2+} imaging strategy to visualize activity of excitatory interneurons and projection neurons within the superficial dorsal horn.

B) Representative image of excitatory spinal cord dorsal horn neurons labeled with GCaMP6s (green), including DiI-backlabeled spinoparabrachial neurons (SPBNs) (red). Scale bar, 50 um.

C) Schematic and representative image of targeting the lateral parabrachial nucleus (lPBN) with the retrograde label DiI, Scale bar, 50 μm.

D) Schematic of the multiplane Ca^{2+} imaging approach. 5 separate optical planes with a spacing of 15 μm are imaged simultaneously, capturing neurons throughout lamina I and II.

E) Schematic of the direct and downstream populations activated in response to bath application of GRP, octreotide, and SP. SSTR is expressed within inhibitory dorsal horn neurons and thus we recorded neurons that are downstream of SSTR neurons only.
F) Representative ΔF/F Ca^{2+} traces from neurons showing network level responses to 300 nM GRP.
G) Representative ΔF/F Ca^{2+} traces from neurons showing network level responses to 200 nM octreotide.
H) Representative ΔF/F Ca^{2+} traces from neurons showing network level responses to 1uM SP.
I) Schematic showing that the Ca^{2+} activity of both interneurons (INs) and SPBNs was analyzed in panels J-L.
J) Percentage of excitatory superficial dorsal horn neurons activated by GRP over time (left y-axis) and total percentage of neurons that showed any activity in response to GRP (right y-axis) (n= 219-610 total neurons/mouse, N=3 mice). Data are shown as mean ± SEM.
K) Percentage of excitatory superficial dorsal horn neurons activated by octreotide over time (left y-axis) and total percentage of neurons that showed any activity in response to octreotide (right y-axis) (n= 219-610 total neurons/mouse, N=3 mice). Data are shown as mean ± SEM.
L) Percentage of excitatory superficial dorsal horn neurons activated by SP over time (left y-axis) and total percentage of neurons that showed any activity in response to SP (right y-axis) (n= 186-450 total neurons/mouse, N=5 mice). Data are shown as mean ± SEM.
M) Schematic showing that only the Ca^{2+} activity of SPBNs was analyzed in panels N-P.
N) Percentage of SPBNs activated by GRP over time (left y-axis) and total percentage of SPNs that showed any activity in response to GRP (right y-axis) (n= 6-14 SPBNs/mouse, N=3 mice). Data are shown as mean ± SEM.
O) Percentage of SPBNs activated by octreotide over time (left y-axis) and total percentage of SPBNs that showed any activity in response to octreotide (right y-axis) (n= 5-14 SPBNs/mouse, N=3 mice). Data are shown as mean ± SEM.
P) Percentage of SPBNs activated by SP over time (left y-axis) and total percentage of SPNs that showed any activity in response to SP (right y-axis) (n= 1-14 SPBNs/mouse, N=3 mice). Data are shown as mean ± SEM.
Q) Agonists targeting GRPR (295 ng GRP), NK1R (400 ng SP), or SSTR (30 ng octreotide) were administered intrathecally and spontaneous scratching was quantified in 5-min bins.
R) Time course of scratching (left y-axis) and total scratches (right y-axis) following intrathecal injection of GRP (N=15 mice). Data are shown as mean ± SEM.
S) Time course of scratching (left y-axis) and total scratches (right y-axis) following intrathecal injection of octreotide (N=8 mice). Data are shown as mean ± SEM.
T) Time course of scratching (left y-axis) and total scratches (right y-axis) following intrathecal injection of Substance P (N=10 mice). Data are shown as mean ± SEM.

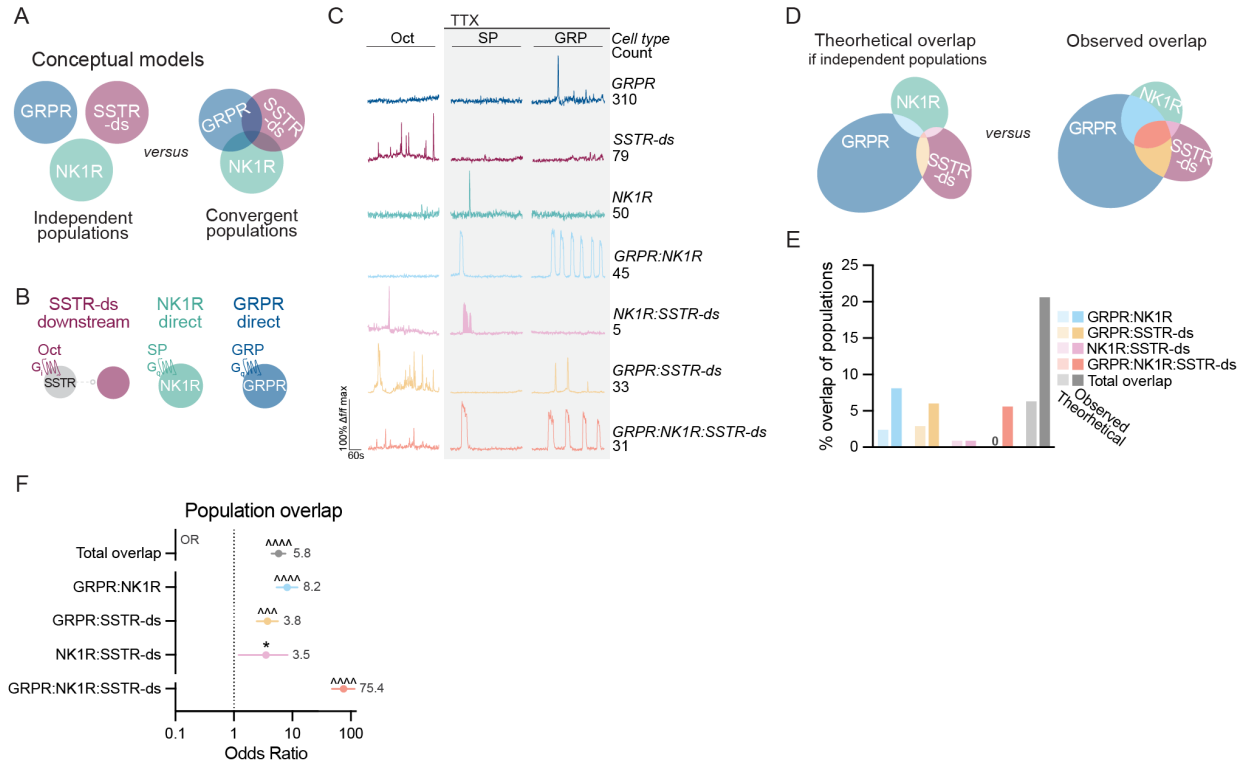

Figure 2. Diverse itch-causing peptides engage a convergent spinal neuron population

A) Models for how diverse itch-causing peptides culminate in scratching behavior. (Left) Different peptides engage independent populations of neurons. (Right) Different peptides engage a convergent population of neurons.

B) Schematic of cell types visualized upon application of octreotide (200 nM) in the absence of TTX (SSTR-ds) and application of SP (1uM) or GRP (300 nM) in the presence of TTX (500 nM) (NK1R direct, GRPR direct).

C). Representative Ca^{2+} imaging traces and cell counts of neurons that responded to one or multiple itch peptides.

D) Euler diagram of (left) the extent of population overlap predicted if peptides acted on independent populations of neurons, versus (right) the observed overlap of neurons activated by each peptide.

E) Of neurons that responded to itch peptides, the theoretical overlap between populations if populations were independent, compared to the observed overlap between populations.

F) GRPR, NK1R, and SSTR populations overlap at frequencies much higher than expected by the prevalence of each cell type (n=3367 total neurons, n=236-599 neurons/mouse, N=8 mice). Odds ratio (OR) analyses, Bonferroni correction for multiple comparisons. OR values for each cell type in gray. Data are shown as OR estimate ± upper and lower 95% CI.

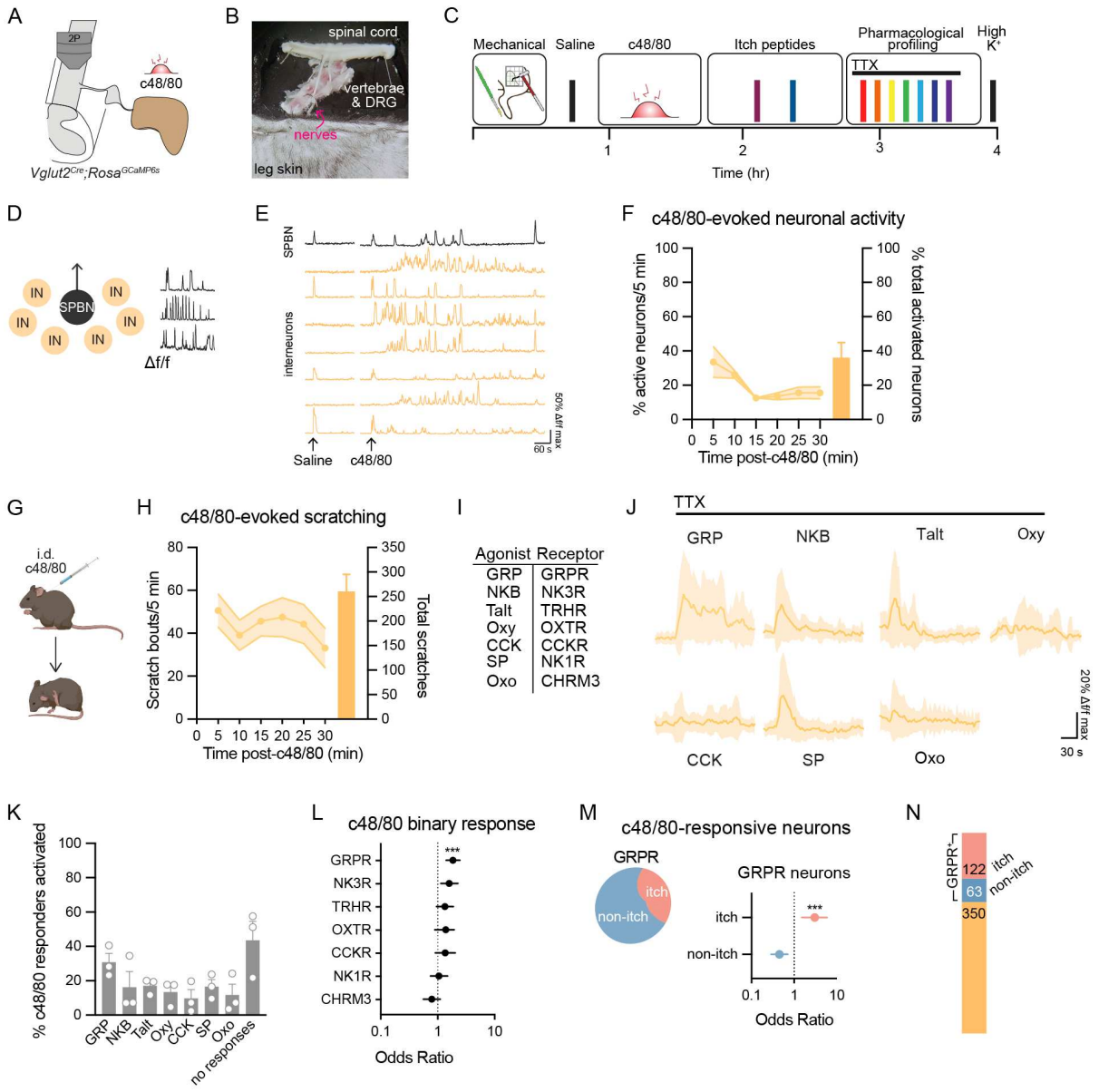

Figure 3. GRPR spinal neurons encode responses to cutaneous pruritogens

A) Experimental strategy for visualizing activity evoked in excitatory superficial dorsal horn neurons caused by intradermal injection of compound 48/80 (91 µg).

B) Image of the *ex vivo* semi-intact somatosensory preparation.

C) Experimental timeline for visualizing activity evoked by intradermal injection of compound 48/80, itch peptides, as well as pharmacological profiling of excitatory superficial dorsal horn neurons.

D) Schematic showing that Ca^{2+} activity of both interneurons (INs) and SPBNs was analyzed in panels E-F.

E) Representative ΔF/F Ca^{2+} traces from individual neurons that responded to intradermal injection of compound 48/80.

F) Percentage of excitatory superficial dorsal horn neurons activated by compound 48/80 over time (left y-axis), and total percentage of neurons that showed any activity in response to

compound 48/80 (right y-axis) (n= 354-610 total neurons/mouse, N=3 mice). Data are shown as mean ± SEM.
G) Compound 48/80 (91 µg) was administered intradermally and scratching was quantified in 5-min bins.
H) Time course of scratching (left y-axis) and total scratches (right y-axis) following intradermal injection of compound 48/80 (N=11 mice). Data are shown as mean ± SEM.
I) Ligands used to pharmacologically profile spinal neuron populations and their cognate G_q-coupled receptors.
J) Representative normalized ΔF/F Ca^{2+} traces from experiments pharmacologically profiling compound 48/80-activated neurons. Only neurons that responded to at least 1 ligand were included. Each cell's ΔF/F trace was normalized to a maximum of 1 and a minimum of 0 (n=44 neurons, N=1 mouse). Data are shown as mean ± SEM.
K) Percentage of compound 48/80-responsive neurons that also respond to application of ligands for pharmacological profiling (n=85-325 compound 48/80-responsive neurons, N=3 mice). Data are shown as mean ± SEM.
L) GRPR is the only receptor associated with whether a neuron will respond to compound 48/80 (n=85-325 compound 48/80-responsive neurons, N=3 mice). Data are shown as odds ratio estimate ± upper and lower 95% CI.
M) GRPR itch neurons are more likely to respond to compound 48/80 than GRPR non-itch neurons. Data are shown as odds ratio estimate ± upper and lower 95% CI.
N) Quantification of the number of compound 48/80-responsive neurons that are GRPR itch neurons, GRPR non-itch neurons, or lack GRPR. n = 535 compound 48/80 neurons pooled from N=3 mice. GRPR itch neurons are defined as those that respond to at least 1 other itch peptide.

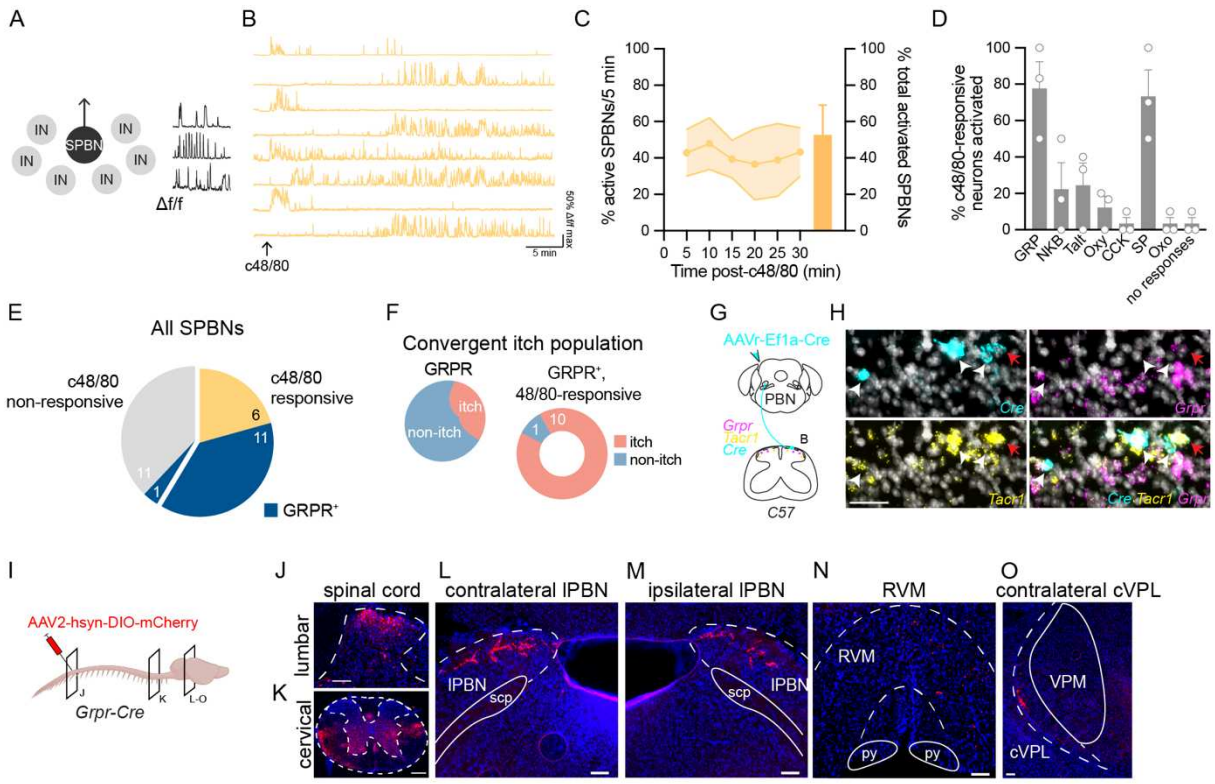

Figure 4. GRPR spinoparabrachial neurons convey itch to the brain

A) Schematic showing that the Ca^{2+} activity of SPBNs was specifically analyzed in panels B-F.

B) Representative ΔF/F Ca^{2+} traces from individual SPBNs that responded to intradermal injection of compound 48/80.

C) Percentage of SPBNs activated by compound 48/80 over time (left y-axis), and total percentage of SPBNs that showed any activity in response to compound 48/80 (right y-axis) (n= 5-14 PBNs/mouse, N=3 mice). Data are shown as mean ± SEM.

D) Percentage of compound 48/80-responsive SPBNs that responded to application of ligands for pharmacological profiling (n=1-10 compound 48/80-responsive SPBNs, N=3 mice). Data are shown as mean ± SEM.

E) GRPR is enriched in SPBNs that respond to compound 48/80 responsive relative to those that do not respond to compound 48/80 (n=29 SPBNs pooled from N=3 mice).

F) GRPR SPBNs that respond to compound 48-80 are GRPR itch neurons (n=11 $GRPR^+$ compound 48/80 responsive SPBNs pooled from N=3 mice).

G) Strategy to retrogradely label SPBNs and visualize them with fluorescent *in situ* hybridization (FISH).

H) Representative image of FISH of the superficial dorsal horn showing retrogradely labeled SPBNs (Cre, white arrowheads) that express *Grpr*, *Tacr1*, or both transcripts (red arrows). Scale bar, 50 μm.

I) Strategy for anterogradely labeling GRPR SPBNs and visualizing their central projections using *Grpr-Cre* mice.

(J and K) Representative labeling of *Grpr-Cre* cell bodies at the site of viral injection in the lumbar spinal cord and ascending axons in the cervical spinal cord. Scale bars, 50 μm and 500 μm, respectively.

(L-O) Representative images of *Grpr-Cre* spinal projection neuron processes targeting the contralateral lPBN, ipsilateral lPBN, RVM, and contralateral cVPL. Scale bars, 50 μm.

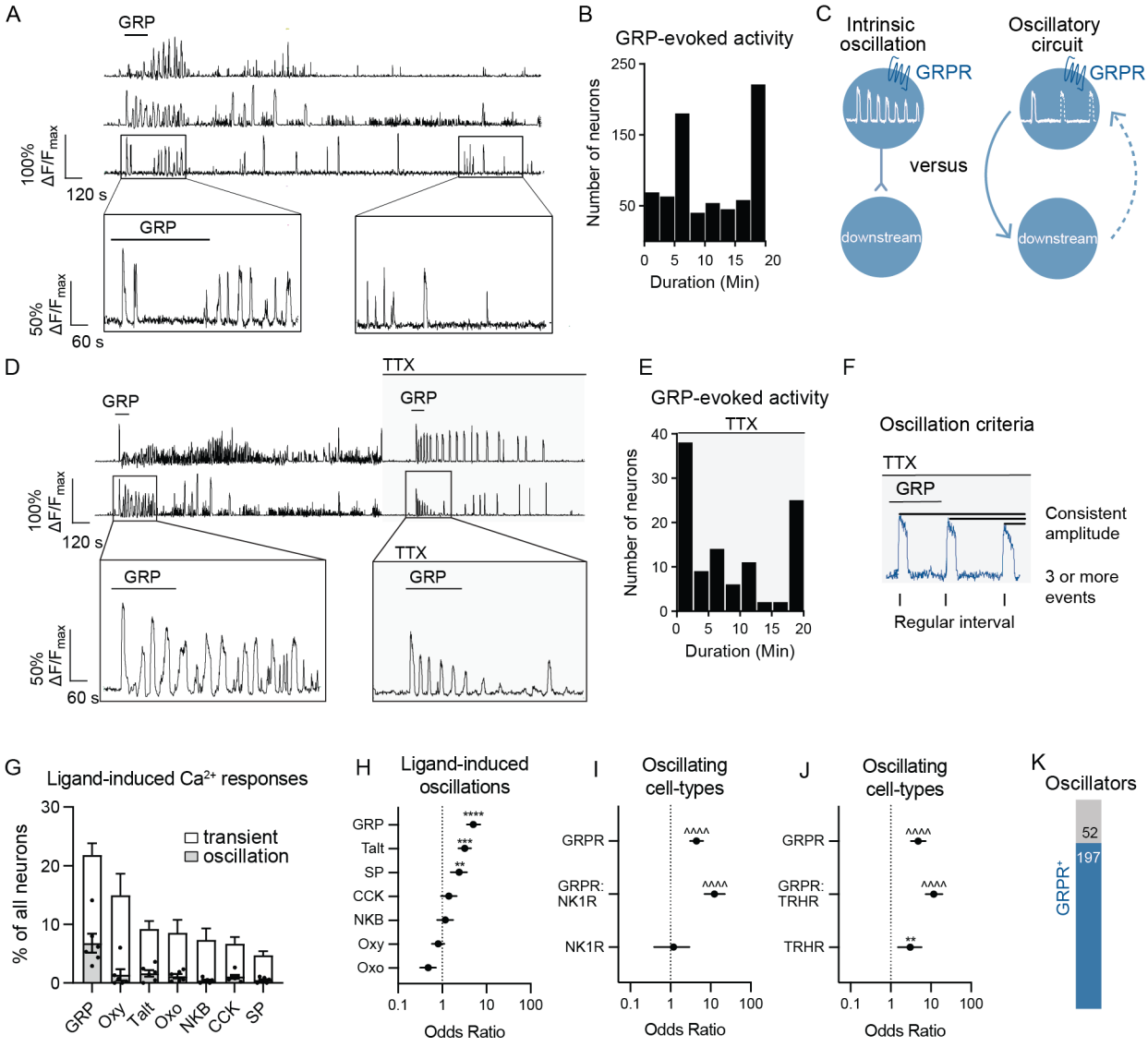

Figure 5. GRPR neurons can display persistent, cell-intrinsic Ca^{2+} oscillations

A) Representative ΔF/F Ca^{2+} traces from neurons showing GRP-induced repeated transients that persist long after GRP washout.

B) Duration (min) of GRP-evoked activity (n= 730 total neurons, n=111-447 neurons/mouse, N=3 mice).

C) Models for how oscillations could occur in response to GRP. (Left) Oscillations may be an intrinsic feature of GRPR neurons (intrinsic oscillation), or GRPR neurons may form positive feedback loops with downstream neurons to maintain oscillation (oscillatory circuits).

D) Representative ΔF/F Ca^{2+} traces from neurons showing that GRP application evokes prolonged oscillations in both the absence (left) and presence (right) of TTX (500 nM, 8 min pretreatment).

E) Duration of GRP-evoked activity in the presence of TTX (n= 56 total neurons, n=26-30 neurons/mouse, N=2 mice).

F) Schematic showing criteria for defining Ca^{2+} oscillations. Oscillation was defined as 3 or more Ca^{2+} transients that occur in regular intervals and have consistent amplitudes in the presence of TTX.

G) Percentage of neurons that displayed Ca^{2+} transients versus Ca^{2+} oscillations in response to GPCR ligands applied in the presence of TTX (n=275-694 total neurons/mouse from N=6 mice). Data are shown as mean ± SEM, with closed circles representing percentage of cells that oscillate to the ligand in each individual mice.
H) GRP, Talt, and SP are all ligands that induce oscillations in neurons. (n=101-370 ligand-responsive neurons/mouse, N=6 mice). Data are shown as OR estimate ± upper and lower 95% CI.
I and J) GRPR expression is the defining feature of cell-types that display cell-intrinsic Ca^{2+} oscillations (n=26- 66 oscillating neurons/mouse, N=6 mice). Data are shown as OR estimate ± upper and lower 95% CI.
K) GRPR is expressed in the majority of neurons that display cell-intrinsic Ca^{2+} oscillations (n=249 oscillating neurons pooled neurons from N=6 mice).